

A platinum shell for ultraslow ligand exchange: unmodified DNA adsorbing more stably on platinum than thiol and dithiol on gold

Wenhu Zhou,^{a,b} Jinsong Ding^{a*} and Juwen Liu^{a,b*}

Received 00th January 20xx,
Accepted 00th January 20xx

DOI: 10.1039/x0xx00000x

www.rsc.org/

Due to the ultraslow ligand exchange rate on Pt, non-thiolated DNA is adsorbed on platinum NPs (PtNPs) more stably than thiolated and even dithiolated DNA on AuNPs. Adsorption kinetics, capacity and stability are systematically compared as a function of DNA sequence. The Pt conjugates can tolerate extreme pH, salt, and thiol molecules. Taking advantage of the optical property of AuNPs and extremely stability of DNA on PtNPs, Au@Pt NPs are prepared, allowing a cost-effective and more stable bioconjugation method. DNA-directed assembly of non-thiolated DNA conjugates is also demonstrated.

DNA-functionalized nanomaterials have tremendously fueled the growth of nanobiotechnology in the past two decades.¹ A key step is bioconjugation of DNA. DNA is attached either via physisorption or a covalent linkage.² While covalent attachment affords higher stability and better control over DNA orientation, adsorption of unmodified DNA is simpler and more cost-effective. Till date, however, there are no such examples testifying that an unmodified DNA can achieve sufficiently high adsorption stability comparable to those by DNA modified with a thiol or amino group.

Attaching DNA to gold nanoparticles (AuNPs) illustrates this point very well.^{1h,2a,3} Spectroscopic studies indicated that unmodified DNA can be adsorbed by gold via base coordination.⁴ The affinity is quite high for all the four bases (>100 kJ/mol in vacuum), especially with adenine.⁵ Various methods have been developed to achieve selective attachment of unmodified DNA to AuNPs.^{2b,c,6} The long-term stability, however, is still lower than that of thiolated DNA.

Adsorption stability depends on two parameters: adsorption energy and ligand exchange rate. So far, most studies are focused on the former.⁷ We reason that new properties and insights might be achieved by taking advantage of the ligand exchange kinetics. Ligand exchange rate is related to desorption activation energy. If metals with slower ligand exchange rates are used, it might be possible to obtain stable attachment even with unmodified DNA.

Platinum is known to have very slow ligand exchange rates. For

example, the aqua ligand exchange rates of Pt²⁺ and Pt⁴⁺ are 10⁻³ and 10⁻⁵ s⁻¹, respectively, while most of the first row transition metals are between 10⁴ to 10⁷ s⁻¹.⁸ Therefore, the difference can reach 12 orders of magnitude. In addition, the action mechanism of cisplatin is believed to be related to the slow ligand exchange rate of Pt when coordinated with DNA (e.g. the time scale of ligand exchange is comparable with the cell cycle).⁹ Given these facts, we hypothesize that ligand exchange on platinum nanoparticles (PtNPs) might also be very slow, allowing unmodified DNA to be stably attached.

A few studies involving DNA-functionalized PtNPs were reported for electrochemical signaling,¹⁰ and directed assembly.¹¹ The adsorption of DNA bases by PtNPs is also known.¹² However, the majority of these works still followed the methods and logic used for adsorbing thiolated DNA on AuNPs, without considering the slow ligand exchange property of platinum. Herein, we communicate a quite striking finding that adsorption of even DNA thymine base (the weakest among the four bases) on PtNP is more stable than thiolated and dithiolated DNA adsorption on AuNPs. On PtNPs, kinetics dominate thermodynamic factors and this is very different from that of AuNPs. To still take advantage of the unique plasmonic property of AuNPs, we made a gold core and platinum shell nanoparticle (Au@Pt) for DNA-directed assembly using unmodified DNA.

Our PtNPs were prepared by reducing Na₂PtCl₆ in the presence of citrate following a literature reported method.¹³ Citrate is a good ligand for Pt,¹⁴ allowing charge stabilization. Dynamic light scattering (DLS) indicated an average hydrodynamic size of ~5 nm (Figure 1A) and this was confirmed by TEM (inset). Zeta-potential measurement shows a negatively charged surface (-20.6 mV), which is consistent with citrate capping. The concentration of our as-synthesized PtNPs is ~60 nM.

To have a complete understanding, we first studied DNA adsorption as a function of salt concentration using a non-thiolated 12-mer DNA bearing a terminal Alexa Fluor 488 (AF) label. Similar to AuNPs, PtNPs are also strong fluorescence quenchers, allowing convenient monitoring of DNA adsorption (Figure 1B). Without additional salt, the fluorescence was stable (Figure 1C), indicating the lack of DNA adsorption. The adsorption rate gradually accelerated with increasing salt concentration because of charge screening. However, the rate of adsorption was still quite slow even with 300 mM NaCl. We previously reported that DNA adsorption by AuNPs is significantly enhanced at low pH,¹⁵ and indeed this was

^a School of Pharmaceutical Sciences, Central South University, Changsha, Hunan 410013, China. Email: dingjs0221@163.com

^b Department of Chemistry and Waterloo Institute for Nanotechnology, University of Waterloo. E-mail: liujw@uwaterloo.ca; Fax: +1 519 7460435; Tel: +1 519 8884567 Ext. 38919

† Electronic Supplementary Information (ESI) available: See DOI: 10.1039/x0xx00000x

also observed with PtNPs (Figure 1D). At pH 3, saturated adsorption was achieved in just 10 min.

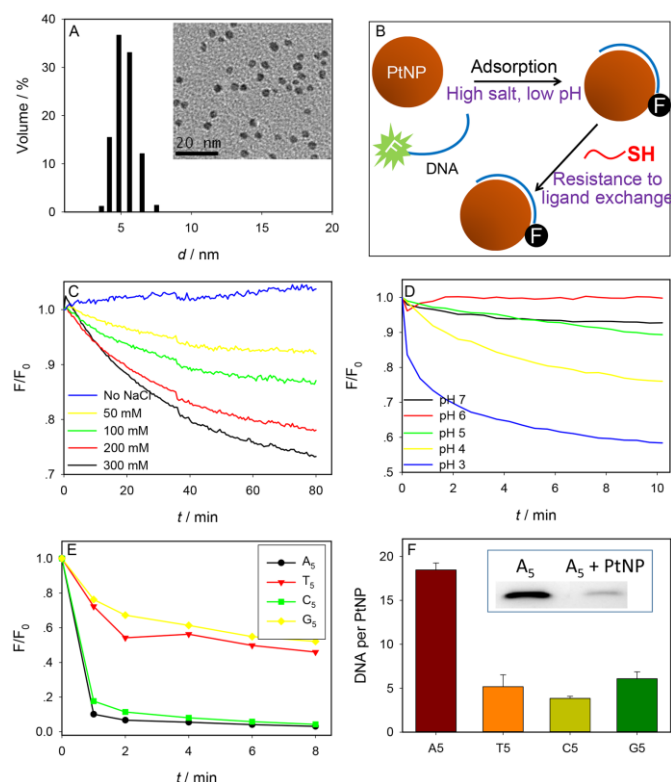


Figure 1. (A) Dynamic light scattering (DLS) and TEM micrograph (inset) of 5 nm PtNPs. (B) A scheme of fluorescently labeled DNA adsorption by PtNP and fluorescence quenching. Once adsorbed, even thiol cannot displace the DNA. Adsorption kinetics of the AF-labeled DNA by PtNPs as a function of (C) NaCl concentration at pH 6 and (D) pH. (E) Adsorption kinetics and (F) adsorption capacity of 5-mer FAM-labeled DNA as a function of DNA sequence at pH 3. Inset of (F): a gel image showing the method of quantification of adsorbed DNA. After adding PtNPs, the band intensity decreases due to DNA adsorption.

Next the effect of DNA sequence was studied. To understand the effect of different bases, 5-mer FAM (carboxyfluorescein)-labeled DNA homopolymers were employed (DNA:PtNP = 5:1). Under this condition, all added DNA can be potentially adsorbed, making kinetic comparison more straightforward. Since FAM is a pH sensitive fluorophore, aliquots of the mixture were transferred at different time points into a pH 7.5 buffer for measurement (Figure 1E). The measured fluorescence intensity is thus proportional to the concentration of non-adsorbed DNA. C₅ and A₅ DNA adsorbed much faster than T₅ and G₅, which is attributed to the protonation of cytosine and adenine at pH 3, thus reducing the negative charge density on DNA. Thymine and guanine cannot be protonated at pH 3, and are less affected by the pH change. We further studied the effect of DNA length and found that poly-A DNA is adsorbed faster than poly-T at all tested lengths (Figure S1).

The DNA loading capacity was next quantified at a higher ratio of 20 (DNA):1 (PtNP) so that the surface can be fully saturated. Since PtNPs cannot be dissolved by KCN, we used gel electrophoresis to quantify adsorbed DNA (inset of Figure 1F). A₅ was adsorbed with the highest density, yielding ~18 DNA per PtNP

(Figure 1F). The capacities of the rest DNAs are quite similar and much lower (~5). G₅ and T₅ are adsorbed more slowly and thus each adsorbed molecule has more time to interact with PtNP surface, resulting in DNA wrapping around the PtNP surface and low capacity. Poly-C DNA tends to form the i-motif structure in acidic solutions, which may contribute to its lower capacity.¹⁶ Poly-A DNA is adsorbed very quickly without forming rigid complex structures like in poly-C. Therefore, more A₅ molecules were adsorbed. These experiments indicate that in terms of DNA adsorption kinetics and capacity, the surface properties of Pt and Au are quite similar.^{2c,6b} However, as described below, the adsorption stability is very different.

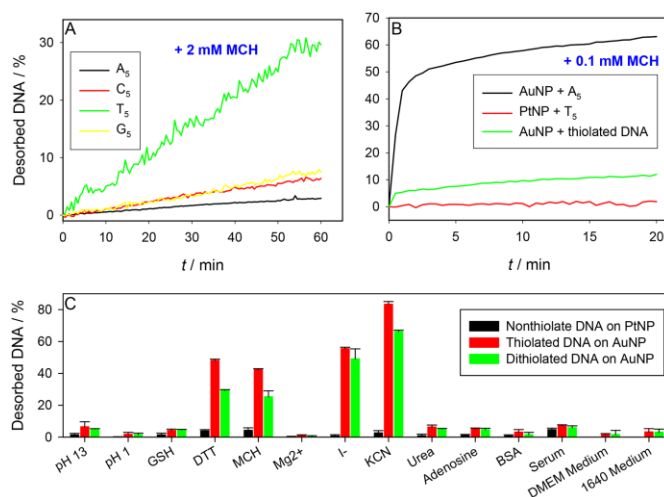


Figure 2. (A) Desorption kinetics of FAM-labeled nonthiolated DNA from PtNPs after treatment with 2 mM MCH. (B) DNA desorption kinetics from AuNPs and PtNPs after treatment with 0.1 mM MCH. (C) DNA desorption percentage (see Table S1 for sequences, DNAs 2-4 used here) from AuNPs and PtNPs under various conditions ([GSH] = 2 mM, [DTT] = 2 mM, [MCH] = 2 mM, [Mg²⁺] = 50 mM, [KI] = 20 mM, [KCN] = 10 mM, [Urea] = 160 mM, [Adenosine] = 1 mM, [BSA] = 1%).

The main assumption of this work is that a Pt surface may offer higher DNA adsorption stability. To test this, a few DNA conjugates were challenged under harsh conditions. First, the four FAM-labeled non-thiolated DNAs were loaded on the PtNPs. After removing free DNA by centrifugation, the conjugates were exposed to 2 mM mercaptohexanol (MCH), which is much more concentrated compared to the DNA in the system (only ~0.3 μM). Out of the four DNAs, only FAM-T₅ desorbed ~30% after 1 h (Figure 2A), while the FAM-A₅ desorbed only ~2% within the same time period. For comparison, when FAM-A₅ was attached to AuNPs, 60% of the DNA were quickly desorbed with only 0.1 mM MCH (Figure 2B, black curve). Even thiolated DNA desorbed ~10% from AuNPs with 0.1 mM MCH (green curve), while the FAM-T₅ DNA remained stable on PtNPs under this condition (red curve). Therefore, even the weakest base thymine is more stably adsorbed on Pt than the adsorption of thiolated DNA on AuNPs. Similar observations were made with nucleoside displacement (Figure S2), where free nucleosides cannot displace adsorbed DNA. Next, we compared a non-thiolated DNA (DNA4, see Table S1 for sequence) on PtNPs with DNA of the same sequence containing a thiol (DNA2) and a dithiol (DNA3) on AuNPs under various conditions, including extreme pH, thiol, salt, strong ligands (I⁻, CN⁻), denaturing agents (urea), nucleosides and cell culture medium (Figure 2C). After 1 h incubation, less than 5% DNA

was desorbed from PtNPs under any tested condition, which further confirms the high stability of DNA adsorption on PtNPs. On the other hand, the thiolated and even dithiolated DNA^{7a} desorbed significantly more, especially in the presence of strong ligands.

These observations have non-trivial implications. First, attaching DNA to PtNPs is sufficient by just using DNA base adsorption and there is no need to add an additional thiol. This is different from gold, where thiol is required to withstand harsh conditions. The PtNP conjugate stability is so high that it outperforms dithiolated DNA on AuNP. Second, this high stability is not only associated with high adsorption energy, but more importantly, with slow ligand exchange rate. For example, if the surface of the PtNPs is capped by thiol first, DNA fails to adsorb (Figure S3). Therefore, this system is under strong kinetic control. Ligands adsorbed first have the advantage. It needs to be noted that weak ligands such as citrate can still be displaced. Third, this conjugate chemistry might be applied to other materials by coating a Pt shell (vide infra).

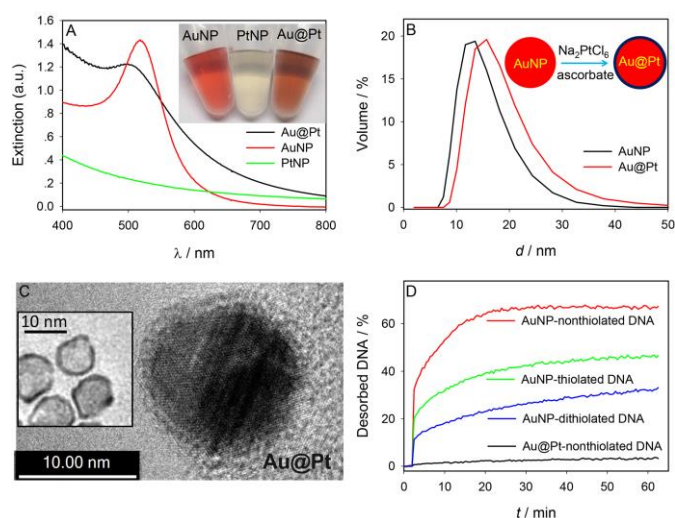


Figure 3. (A) UV-vis spectra and photographs (insert) of AuNPs, PtNPs and Au@Pt NPs. (B) DLS of AuNPs and Au@Pt NPs. Inset shows the scheme of synthesis. (C) High resolution TEM micrograph of an Au@Pt NP. Inset is the TEM micrograph of the sample after KCN treatment showing the Pt shell with the Au core dissolved. (D) DNA desorption kinetics from AuNP and Au@Pt NP after treatment with 50 μ M (AuNP) or 1 mM (Au@Pt NP) MCH. DNAs 2-4 were used here.

While PtNPs have excellent adsorption stability, it lacks the unique optical property of AuNPs. For example, PtNPs are brown and do not display any characteristic extinction peaks in the visible region (Figure 3A, green line). For comparison, AuNPs are red in color (Figure 3A, red line). We hypothesize that Au core Pt shell NPs (Au@Pt) might combine the optical property of Au and the adsorption stability of Pt. Using 13 nm AuNPs as seeds, we grew a thin layer of Pt on their surface.¹⁷ The color of the resulting hybrid material turned to dark red and the 520 nm plasmon peak of gold was slightly broadened (Figure 3A, black line). DLS showed the shift of the AuNP peak from 13 nm to 16 nm (Figure 3B), suggesting that the Pt layer is \sim 1.5 nm thick. DLS also indicated that the particles were stable and did not aggregate during synthesis. High resolution TEM shows a uniform coating of crystalline Pt layer with a thickness of \sim 2 nm (Figure 3C). When KCN was added to dissolve the gold

core, a Pt shell is produced (inset of Figure 3C), confirming the core/shell structure.

To test whether this thin Pt shell is sufficient to maintain the adsorption stability, we then challenged its DNA conjugate with MCH (Figure 3D). The non-thiolated DNA did not release from the Au@Pt surface, while non-thiolated, thiolated and even dithiolated DNA were released from the AuNPs. Note that the MCH concentration for PtNP was 20 times higher than that of AuNP in this test. Therefore, a thin shell of Pt is sufficient to support stable DNA adsorption.

This high adsorption stability and slow ligand exchange rate may also cause problems for selective DNA attachment. The system is under strong kinetic control. If a DNA is attached with a certain conformation on PtNP, it is very difficult to correct it. This is different from AuNPs, where two-step attachment can take place using a thiolated DNA. First, both the thiol and base adsorption can take place at low DNA coverage. Then, thiol can displace DNA bases at high DNA coverage.^{4a} This process is called salt aging if the high DNA coverage is enabled by adding salt.^{2d} This is because thiol adsorption is thermodynamically more stable and the ligand exchange rate is relatively fast. In the case of PtNP, it is unclear whether thiol adsorbs more stably than DNA bases or not,¹⁸ but both are sufficiently stable and it is very difficult to displace one with the other. Deng and co-workers used a phosphine ligand to cap PtNPs and then added a duplex thiolated DNA, which allowed attachment via the two thiol ends.¹¹

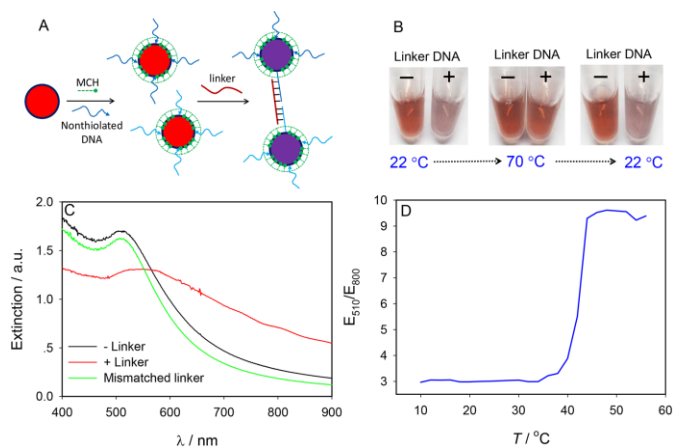


Figure 4. (A) Scheme of DNA attachment to Au@Pt NPs and DNA-directed Au@Pt NP assembly. These nonthiolated DNAs contain a poly-A block for anchoring on the particle surface. To minimizing non-specific adsorption, MCH was also included for this step. (B) Photographs showing reversible aggregation and melting of DNA-linked Au@Pt NPs. (C) UV spectra of DNA-linked Au@Pt NPs aggregation. (D) A melting curve of DNA-linked Au@Pt NPs.

Our goal is to employ only non-thiolated DNA. After trying a few different conditions, we have developed a method to kinetically control DNA adsorption via co-adsorption of a small alkylthiol molecule (Figure 4A). Two different DNAs were used to respectively functionalize two batches of Au@Pt NPs. These DNAs contain a block of adenine intended for anchoring on the Au@Pt NP surface. DNA and MCH were simultaneously added at a ratio of 20:1. Since MCH diffuses faster and is likely to reach the particle surface first, it was only used at a trace amount. The adsorbed MCH serves as pillows on the surface to prevent the subsequently adsorbed DNA

from lying flat on the Au@Pt NP surface. Then pH was then adjusted to 3 to allow DNA adsorption. Afterwards, the rest of the Au@Pt NP surface was fully capped with MCH by adding an excess amount of MCH. After removing the free DNA, the resulting conjugate maintained excellent colloidal stability. After mixing two types of particles and linker DNA as show in Figure 4A, the color of the system changed to purple, indicating plasmonic coupling and NP assembly (Figure 4B). When heated to 70 °C, the color changed back to red, and when cooled down to room temperature the color is changed to purple again. This color change is also reflected from the UV-vis spectroscopy (Figure 4C). A control experiment was also performed using the same process but with a 24-mer non-complementary control DNA. No obvious UV spectrum change was observed (Figure 4C, green spectrum). The sharp melting curve also indicates a cooperative melting transition characteristic of DNA-directed assembly (Figure 4D).¹⁹

In conclusion, we reported the ultrahigh stability of non-thiolated DNA adsorption by PtNPs. This stability is attributed to the extremely slow ligand exchange rate related to Pt, which is an intrinsic property of this metal. Adsorption of even the weakest thymine is much stronger than adsorption of thiolated and even dithiolated DNA on AuNPs. By coating AuNPs with a thin shell of Pt, we combined both the optical property of gold and the adsorption stability of Pt. The resulting conjugate is functional and undergoes reversible DNA-directed assembly. While most of the previous work was focused on adsorption energy or using covalent conjugation methods, this study has provided a deep understanding on ligand exchange on metallic nanoparticle surfaces. By using non-thiolated DNA, the cost of conjugate preparation can be reduced significantly and it will make the technology available for a broader research community. With this ultra-stable conjugate, new applications in challenging environment may also be enabled.

This work is supported by the University of Waterloo, the Natural Sciences and Engineering Research Council of Canada (NSERC), Foundation for Shenghua Scholar of Central South University and the National Natural Science Foundation of China (Grant No. 21301195). W. Zhou is supported by a Fellowship from the China Scholarship Council (CSC, Grant No. 201406370116).

Notes and references

- (1) (a) Park, S. Y.; Lytton-Jean, A. K. R.; Lee, B.; Weigand, S.; Schatz, G. C.; Mirkin, C. A. *Nature* **2008**, *451*, 553;(b) Nykypanchuk, D.; Maye, M. M.; van der Lelie, D.; Gang, O. *Nature* **2008**, *451*, 549;(c) Pinheiro, A. V.; Han, D.; Shih, W. M.; Yan, H. *Nat. Nanotechnol.* **2011**, *6*, 763;(d) Tan, S. J.; Campolongo, M. J.; Luo, D.; Cheng, W. *Nat Nanotechnol.* **2011**, *6*, 268;(e) Wang, H.; Yang, R. H.; Yang, L.; Tan, W. H. *ACS Nano* **2009**, *3*, 2451;(f) Song, S. P.; Qin, Y.; He, Y.; Huang, Q.; Fan, C. H.; Chen, H. Y. *Chem. Soc. Rev.* **2010**, *39*, 4234;(g) Liu, J.; Cao, Z.; Lu, Y. *Chem. Rev.* **2009**, *109*, 1948;(h) Zhao, W.; Brook, M. A.; Li, Y. *ChemBioChem* **2008**, *9*, 2363;(i) Katz, E.; Willner, I. *Angew. Chem. Int. Ed.* **2004**, *43*, 6042;(j) Giljohann, D. A.; Seferos, D. S.; Daniel, W. L.; Massich, M. D.; Patel, P. C.; Mirkin, C. A. *Angew. Chem. Int. Ed.* **2010**, *49*, 3280;(k) Lan, X.; Lu, X.; Shen, C.; Ke, Y.; Ni, W.; Wang, Q. *J. Am. Chem. Soc.* **2014**, *137*, 457.
- (2) (a) Saha, K.; Agasti, S. S.; Kim, C.; Li, X.; Rotello, V. M. *Chem. Rev.* **2012**, 2739–2779;(b) Pei, H.; Li, F.; Wan, Y.; Wei, M.; Liu, H.; Su, Y.; Chen, N.; Huang, Q.; Fan, C. *J. Am. Chem. Soc.* **2012**, *134*, 11876;(c) Zhang, X.; Liu, B.; Dave, N.; Servos, M. R.; Liu, J. *Langmuir* **2012**, *28*, 17053;(d) Cutler, J. I.; Auyeung, E.; Mirkin, C. A. *J. Am. Chem. Soc.* **2012**, *134*, 1376;(e) Faulds, K.; McKenzie, F.; Smith, W. E.; Graham, D. *Angew. Chem. Int. Ed.* **2007**, *46*, 1829;(f) Sharma, J.; Chhabra, R.; Andersen, C. S.; Gothelf, K. V.; Yan, H.; Liu, Y. *J. Am. Chem. Soc.* **2008**, *130*, 7820;(g) Lan, X.; Chen, Z.; Liu, B. J.; Ren, B.; Henzie, J.; Wang, Q. *Small* **2013**, *9*, 2308.
- (3) (a) Liu, J. *Phys. Chem. Chem. Phys.* **2012**, *14*, 10485;(b) Rosi, N. L.; Mirkin, C. A. *Chem. Rev.* **2005**, *105*, 1547.
- (4) (a) Herne, T. M.; Tarlov, M. J. *J. Am. Chem. Soc.* **1997**, *119*, 8916;(b) Kimura-Suda, H.; Petrovykh, D. Y.; Tarlov, M. J.; Whitman, L. J. *J. Am. Chem. Soc.* **2003**, *125*, 9014.
- (5) Demers, L. M.; Oestblom, M.; Zhang, H.; Jang, N.-H.; Liedberg, B.; Mirkin, C. A. *J. Am. Chem. Soc.* **2002**, *124*, 11248.
- (6) (a) Opdahl, A.; Petrovykh, D. Y.; Kimura-Suda, H.; Tarlov, M. J.; Whitman, L. J. *Proc. Natl. Acad. Sci. USA* **2007**, *104*, 9;(b) Zhang, X.; Liu, B.; Servos, M. R.; Liu, J. *Langmuir* **2013**.
- (7) (a) Li, Z.; Jin, R.; Mirkin, C. A.; Letsinger, R. L. *Nucleic Acids Res.* **2002**, *30*, 1558;(b) Herdt, A. R.; Drawz, S. M.; Kang, Y. J.; Taton, T. A. *Colloids and Surfaces B-Biointerfaces* **2006**, *51*, 130;(c) Bhatt, N.; Huang, P.-J. J.; Dave, N.; Liu, J. *Langmuir* **2011**, *27*, 6132;(d) Li, F.; Zhang, H.; Dever, B.; Li, X.-F.; Le, X. C. *Bioconj. Chem.* **2013**, *24*, 1790.
- (8) Taube, H. *Chem. Rev.* **1952**, *50*, 69.
- (9) (a) Reedijk, J. *Proc. Natl. Acad. Sci. U. S. A.* **2003**, *100*, 3611;(b) Reedijk, J. *Platinum Met. Rev.* **2008**, *52*, 2.
- (10) Polsky, R.; Gill, R.; Kaganovsky, L.; Willner, I. *Anal. Chem.* **2006**, *78*, 2268.
- (11) Li, Y.; Zheng, Y.; Gong, M.; Deng, Z. *Chem. Commun.* **2012**, *48*, 3727.
- (12) Yang, J.; Lee, J.; Too, H.-P.; Chow, G.-M.; Gan, L. J. *Nanopart. Res.* **2006**, *8*, 1017.
- (13) Bigall, N. C.; Härtling, T.; Klose, M.; Simon, P.; Eng, L. M.; Eychmüller, A. *Nano Lett.* **2008**, *8*, 4588.
- (14) Wang, F.; Huang, P.-J. J.; Liu, J. *Chem. Commun.* **2013**, *49*, 9482.
- (15) (a) Zhang, X.; Servos, M. R.; Liu, J. *J. Am. Chem. Soc.* **2012**, *134*, 7266;(b) Zhang, X.; Servos, M. R.; Liu, J. *Chem. Commun.* **2012**, *48*, 10114.
- (16) Choi, J.; Kim, S.; Tachikawa, T.; Fujitsuka, M.; Majima, T. *J. Am. Chem. Soc.* **2011**, *133*, 16146.
- (17) Li, J.-F.; Yang, Z.-L.; Ren, B.; Liu, G.-K.; Fang, P.-P.; Jiang, Y.-X.; Wu, D.-Y.; Tian, Z.-Q. *Langmuir* **2006**, *22*, 10372.
- (18) Reedijk, J. *Chem. Rev.* **1999**, *99*, 2499.
- (19) Jin, R.; Wu, G.; Li, Z.; Mirkin, C. A.; Schatz, G. C. *J. Am. Chem. Soc.* **2003**, *125*, 1643.